



Deposited via The University of Sheffield.

White Rose Research Online URL for this paper:

<https://eprints.whiterose.ac.uk/id/eprint/111164/>

Article:

Domingues, M. M., Macrae, F. L., Duval, C. et al. (2016) Thrombin and fibrinogen gamma ' impact clot structure by marked effects on intrafibrillar structure and protofibril packing. *Blood*, 127 (4). pp. 487-495. ISSN: 0006-4971

<https://doi.org/10.1182/blood-2015-06-652214>

Reuse

Items deposited in White Rose Research Online are protected by copyright, with all rights reserved unless indicated otherwise. They may be downloaded and/or printed for private study, or other acts as permitted by national copyright laws. The publisher or other rights holders may allow further reproduction and re-use of the full text version. This is indicated by the licence information on the White Rose Research Online record for the item.

Takedown

If you consider content in White Rose Research Online to be in breach of UK law, please notify us by emailing eprints@whiterose.ac.uk including the URL of the record and the reason for the withdrawal request.

Thrombin and fibrinogen γ' impact clot structure by marked effects on intrafibrillar structure and protofibril packing

Marco M. Domingues,^{1,2} Fraser L. Macrae,¹ Cédric Duval,¹ Helen R. McPherson,¹ Katherine I. Bridge,¹ Ramzi A. Ajjan,¹ Victoria C. Ridger,³ Simon D. Connell,² Helen Philippou,¹ and Robert A.S. Ariëns¹

¹ Thrombosis and Tissue Repair Group, Division of Cardiovascular and Diabetes Research, Leeds Institute of Cardiovascular and Metabolic Medicine and Multidisciplinary Cardiovascular Research Centre, Faculty of Medicine and Health, University of Leeds, Leeds, UK

² Molecular and Nanoscale Physics group, School of Physics and Astronomy, University of Leeds, Leeds, UK

³ Department of Cardiovascular Science, Faculty of Medicine, Dentistry, and Health, University of Sheffield, Sheffield, UK

Running Title: Thrombin and γ' reduce protofibril packing

Corresponding Author: Dr. Robert Ariëns, Thrombosis and Tissue Repair Group, University of Leeds, LIGHT Laboratories, Clarendon Way, Leeds LS2 9JT, Tel: (+44) 1133437734, Fax: (+44) 1133437738; Email: r.a.s.ariens@leeds.ac.uk.

Word count:

Text – 4,013 (maximum 4,000)

Abstract – 246 (maximum 250)

Tables: 1

Figures: 7 (maximum 7)

References: 49

Key Points

- Thrombin and fibrinogen γ' regulate protofibril packing within fibrin fibers and thereby influence clot stiffness.
- Fibrin analysis after dehydration (e.g. electron microscopy) overestimates changes in fiber size due to effects on protofibril packing.

Abstract

Previous studies have shown effects of thrombin and fibrinogen γ' on clot structure. However, structural information was obtained using electron microscopy, which requires sample dehydration. Our aim was to investigate the role of thrombin and fibrinogen γ' in **modulating** fibrin structure under fully hydrated conditions. Fibrin fibers were studied using turbidimetry, atomic force microscopy, electron microscopy and magnetic tweezers in purified and plasma solutions. Increased thrombin induced a pronounced decrease in average protofibril content per fiber, with a relatively minor decrease in fiber size, leading to the formation of less compact fiber structures. Atomic force microscopy under fully hydrated conditions confirmed that fiber diameter was only marginally decreased. Decreased protofibril content of the fibers produced by high thrombin related to weakened clot architecture as analysed by magnetic tweezers **in purified systems, and by thromboelastometry in plasma and whole blood**. Fibers produced with fibrinogen γ' showed reduced protofibril packing over a range of thrombin concentrations. High magnification electron microscopy demonstrated reduced protofibril packing in γ' fibers and unravelling of fibers into separate protofibrils. Decreased protofibril packing was confirmed in plasma for high thrombin concentrations and fibrinogen-deficient plasma reconstituted with γ' fibrinogen. These findings demonstrate that in fully hydrated conditions, thrombin and fibrinogen γ' have dramatic effects on protofibril content and that **protein density** within fibers correlates with strength of the fibrin network. We conclude that regulation of protofibril content of fibers is an important mechanism by which thrombin and fibrinogen γ' modulate fibrin clot structure and strength.

Introduction

Coagulation culminates in the production of thrombin which converts fibrinogen into fibrin, forming the blood clot, in order to stop bleeding.^{1,2} Fibrinogen is a 340 kDa homodimeric plasma protein consisting of six polypeptide chains (2A α , 2B β and 2 γ) linked together by disulphide bonds.³⁻⁵ A common variant of fibrinogen, fibrinogen γ' ($\gamma A/\gamma'$), is produced by alternative splicing of the γ -chain mRNA.^{6,7} This alternative chain has four C-terminal residues replaced with 20 different residues, with a high proportion of negatively charged residues. Fibrinogen γ' has an average plasma concentration of 8-15%.^{6,8} The $\gamma A/\gamma'$ sequence contains a thrombin binding site, which reduces thrombin inhibition by antithrombin and heparin cofactor II.⁹ On the other hand, binding to fibrinogen $\gamma A/\gamma'$ reduces the availability of thrombin in the circulation, an effect previously described as antithrombin I.¹⁰ We previously found reduced fibrinopeptide (Fp)B but normal FpA release from $\gamma A/\gamma'$ compared with $\gamma A/\gamma A$ fibrin, leading to $\gamma A/\gamma'$ fibrin networks made of thinner fibers and increased branching.¹¹ Increased plasma concentrations of this variant have been associated with cardiovascular conditions such as ischemic stroke,¹² coronary artery disease¹³ and myocardial infarction.¹⁴ Conversely, reduced concentrations have been associated with microangiopathy syndrome¹⁵ and deep vein thrombosis.¹⁶

Fibrinogen shows a trinodular structure with distal D-regions on both ends consisting of the B β - and γ -chain C-terminal domains, while the central E-region comprises the N-terminal sequences of all polypeptide chains.^{3,4} Transmission electron microscopy shows that the α C-terminal regions fold back and interact with the E-region.¹⁷ Thrombin interacts with the E-region to release FpA and FpB, likely disrupting the interaction of the α C-terminus with the E-region.¹⁸ In addition, release of the

fibrinopeptides exposes knobs A and B in the E-region, which interact with their specific binding pockets in the D-regions of another fibrin molecule leading to protofibril formation. Lateral aggregation occurs between the protofibrils which leads to fiber thickening.¹⁹ Variables such as pH, ionic strength,²⁰ fibrinogen²¹, factor XIII²²⁻²⁴ and calcium²⁵ affect clot structure. High concentrations of thrombin^{2,26,27} and prothrombin²⁸ have been reported to lead to thinner and more densely packed fibers, which associate with thrombosis risk.^{29,30}

While previous studies have investigated the effects of thrombin and fibrinogen γ' on the overall network structure of the clot,^{26,31,32} the intrafibrillar structure remains unexplored, and there is little information on the effects of these structural changes on the mechanical properties of fibrin. Therefore, our aim was to investigate the intrafibrillar structure of fibrin under fully hydrated conditions and understand the effects of changes in fiber structure on clot mechanical properties. We found that increasing thrombin concentrations lead to a considerable reduction in the number of protofibrils packed within the fibers, which is associated with reduced clot stiffness in purified systems, plasma and whole blood. We also demonstrate that $\gamma A/\gamma'$ decreases protofibril packing over a range of thrombin concentrations. These data indicate that protofibril packing is a major determinant of clot structure/stiffness and is regulated by both thrombin and fibrinogen γ' .

Methods

Fibrin preparations

In purified systems, clots were prepared in Tris-buffer saline (TBS; 50 mM Tris-HCl, 100 mM NaCl, pH 7.4) with 1 mg.mL⁻¹ (0.5 mg.mL⁻¹ for viscoelasticity measurements) fibrinogen (Merck Millipore, Darmstadt, Germany), 2.5 mM CaCl₂ and 0.005 to 10 U.mL⁻¹ human α -thrombin (Sigma-Aldrich; St Louis, MO). This range was based on thrombin concentrations responsible for key substrate interactions in tissue factor triggered whole blood.³³ Normal pooled plasma was diluted 1/10 in TBS (0.3 mg.mL⁻¹ fibrinogen, measured by ELISA) and supplemented with 10 mM CaCl₂ and 0.1 and 1 U.mL⁻¹ human α -thrombin. Fibrinogen-deficient plasma (Merck Millipore, Darmstadt, Germany) was diluted 1/10, supplemented with different fibrinogen mixtures (100% γ A/ γ A; 60% γ A/ γ A:40% γ A/ γ '; 91% γ A/ γ A:9% γ A/ γ '; 100% γ A/ γ ') at a final concentration of 0.3 mg.mL⁻¹ and the fibrin clot was formed by addition of 0.1 and 1 U.mL⁻¹ α -thrombin and 10 mM CaCl₂.

Turbidimetric analysis of fibrin ultrastructure

See Supplemental Methods for a detailed description of the turbidimetric analysis. In brief, clots were formed in 1 cm polystyrene cuvettes with a final volume of 300 μ L and closed with parafilm to avoid dehydration. The clots were left to form for 24 hours at room temperature before scanning over 500< λ <780 nm (Figure S1) in a Lambda 35 UV-Vis spectrophotometer (Perkin-Elmer; Cambridge, UK). Measurements were performed in triplicate.

Fibrin viscoelasticity

An in-house magnetic tweezers device was used to examine microrheology of fibrin as previously described.^{34,35} Super paramagnetic beads at 1:250 (v/v) (Dynabeads M-450 Epoxy, Invitrogen; Paisley, UK) were trapped by the forming fibrin network in a capillary tube (VitroCom; NJ, USA), and their displacement was measured after 24 hours of clot formation (See Supplemental movie). Both elastic and viscous **shear moduli** were calculated from the time-dependent compliance in order to obtain frequency-dependent moduli.³⁶ Compliance was calculated from the ratio of the time-dependent shear strain (bead displacement) to the magnitude of the force applied. The elastic modulus or clot stiffness, G' , provides information about the energy stored during deformation. The loss modulus or viscous component, G'' , provides information about energy loss during deformation. The loss tangent ($\tan\delta = G''/G'$) was calculated to evaluate the relative ratio between viscous and elastic properties. For a viscous material $\tan\delta \gg 0$ i.e. $G'' \gg G'$, while for an elastic solid $\tan\delta \ll 0$ i.e. $G' \gg G''$. For a viscoelastic material with $\tan\delta = 1$ the amounts of energy dissipated and stored are equal. The values for both G' and G'' were obtained at a frequency of 0.1 Hz. The displacement of 10 random particles were measured per samples and each sample was studied in triplicate.

Atomic Force Microscopy

Atomic force microscopy was used to measure fiber diameters in fully hydrated conditions. Samples were prepared as described by Blinc *et al.*³⁷ Fibrinogen and calcium chloride were premixed in a final volume of 20 μL and transferred to freshly cleaved mica, previously treated with 2 mM NiCl_2 . After addition of human α -thrombin the solution was mixed, and spread on the surface. The sample was

allowed to polymerize for >90 minutes in a humidity chamber, to prevent dehydration. After the clot was fully formed, the sample was rinsed with MilliQ water and washed 5x with TBS. The clot was then immersed in buffer, and imaged in fluid Peak-Force tapping mode with a Nanoscope V MultiMode 8 (Bruker, UK). The images were obtained using a NP-D cantilever ($k=0.06 \text{ N.m}^{-1}$, Bruker; Coventry, UK) with a peak force frequency of 1 kHz, approximately 200 pN, and peak force amplitude of ~60 nm. Image processing and analysis was performed using Nanoscope Analysis v1.5 (Bruker, UK). The radius of each fiber was determined by averaging 5 cross sections at half height of the fiber (Figure S1). Each clotting condition was prepared at least three times, and for each clot, a total of 25 random fibers were measured.

For details regarding normal pooled plasma, [whole blood experiments](#), fibrinogen purification, fibrinogen $\gamma A/\gamma'$ and $\gamma A/\gamma A$ purification, total fibrinogen ELISA, fibrinogen γ' ELISA, [thromboelastometry analysis](#), transmission [electron microscopy](#), scanning [electron microscopy](#) and statistical analysis, see Supplement.

Results

Thrombin reduces fiber radius under dried conditions

The effects of increasing thrombin concentration on fiber radius in fibrin made from human plasminogen-depleted IF-1 purified (which contains both $\gamma A/\gamma A$ and $\gamma A/\gamma'$) fibrinogen in dried conditions are shown in Figure 1. Increasing thrombin concentrations led to increased clot **network** density (Figure 1A) and decreased fibrin fiber radius (Figure 1B). The fiber radius decreased by 1.9 fold (from **63.6±16.7** to **34.3±9.9** nm; $p<0.001$) for thrombin concentrations between 0.1 and 10 U.mL⁻¹.

Thrombin reduces protofibril packing under wet conditions

The effects of thrombin concentration on protofibril packing in wet conditions are shown by turbidimetry in Figure 2. Increasing thrombin concentrations led to decreased fiber radius (Figure 2A) and protofibril **number per fiber** (Figure 2B). Average fiber radius decreased 1.5 fold (from **102.4±0.1** to **68.0±9.8** nm; $p<0.001$), **whereas the number of protofibril packed per fiber cross-section decreased much more and by 4.5 fold (from 294.0±1.4 to 64.9±12.4; $p<0.001$)**, with increasing thrombin. Since the radius did not decrease to the same extent as the protofibril **number**, the protein density **of the fibers** decreased 2.0 fold (Figure 2C). The protofibril distance within fibers increased 1.4 fold at higher compared with lower thrombin concentrations (Figure 2D).

We also studied the effects of thrombin on fibrin intrafibrillar structure in clots produced with plasma (Figure 3). Higher thrombin (1.0 U.mL⁻¹) induced a decrease in the fiber radius of 1.2 fold compared with 0.1 U.mL⁻¹ thrombin (from **88.0±0.5** to **76.5±6.0** nm; Figure 3A), whereas the number of protofibrils packed per fiber was

decreased by as much as 2.4 fold (from 376.9 ± 17.0 to 160.0 ± 33.4 ; $p < 0.005$; Figure 3B). The larger decrease in protofibril number relative to radius led to a 1.8 fold decrease in protein density at 1.0 compared with 0.1 U.mL^{-1} thrombin ($p < 0.005$; Figure 3C). As per corollary, protofibril distance was increased 1.4 fold ($p < 0.001$; Figure 3D).

Atomic force microscopy was used to further investigate the effect of thrombin on fiber size under fully hydrated conditions (Figure 4A). Increasing thrombin decreased the fiber radius modestly and to a similar extent as observed by turbidimetry (1.3-fold decrease from 116.9 ± 35.3 to 87.7 ± 15.4 nm; $p < 0.001$; Figure 4B). The minimum thrombin concentration of 0.1 U.mL^{-1} used in these experiments was chosen as this concentration did not differ from the lowest thrombin concentration (0.005 U.mL^{-1}), when comparing fiber radius by turbidimetry (Figure 2A).

Protofibril packing and clot stiffness

We next investigated the effects of the protofibril packing on clot viscoelastic properties using magnetic tweezers and thromboelastometry. There was a clear tendency towards the formation of fibrin clots that were less stiff with increasing thrombin concentrations in purified systems. At 5.0 U.mL^{-1} thrombin, clot stiffness decreased 2.6 fold compared with 0.1 U.mL^{-1} , as shown by the decrease in the storage modulus G' (Table 1). Thrombin did not affect the energy dissipated within the clot, measured by the loss modulus G'' . The relationship between the loss modulus G'' and storage modulus G' was calculated as the loss tangent, $\tan\delta$, which increased at higher thrombin concentrations. We also performed experiments in the absence of calcium, which showed that G' decreased 1.8 fold while G'' decreased 1.9

fold, with a minor, but not significant, decrease of $\tan\delta$ at higher thrombin concentrations (Table S1).

Effects of thrombin on the elastic properties of clots made with plasma and whole blood were studied using thromboelastometry. While clot formation time was shorter, maximum clot firmness, and consequently storage moduli, were reduced in clots produced with high compared with low thrombin concentrations (Table 2, Figure S5). There were no major differences in clot formation rates between the thrombin concentrations (Table 2). Note that thrombin concentrations in these experiments were higher than in turbidimetric analysis of plasma (Figure 3), since plasma (which contains antithrombin, α 2-macroglobulin and other inhibitors) was diluted 10-fold for turbidimetry but used undiluted for thromboelastometry.

γ A/ γ ' fibrin decreases protofibril packing

We also investigated the effects of thrombin on protofibril packing in clots produced with purified γ A/ γ A and γ A/ γ ' fibrinogen (Figure 5). Increasing thrombin led to a modest decrease in the radius of γ A/ γ A fibers by 1.3 fold (from 104.1 ± 0.4 nm to 83.0 ± 0.5 nm), while for γ A/ γ ' fibers the radius remained unchanged (Figure 5A). At thrombin concentrations below 0.1 U.mL^{-1} , the radius of fibers formed with γ A/ γ A were significantly higher than those produced with γ A/ γ '. At 2 U.mL^{-1} thrombin, the radius of γ A/ γ ' fibers was slightly larger than that of γ A/ γ A. This tendency was maintained for higher thrombin concentrations due to continued decrease of radius for γ A/ γ A fibers and the unchanged radius of γ A/ γ ' fibers. When we analysed protofibril number per fiber, there was a marked difference between γ A/ γ ' and γ A/ γ A

at low thrombin concentrations. At thrombin concentrations $<1 \text{ U.mL}^{-1}$, $\gamma\text{A}/\gamma'$ fibers showed a markedly reduced number of protofibrils (Figure 5B) and protein density (Figure 5C), while the distance between protofibrils was increased (Figure 5D), compared with $\gamma\text{A}/\gamma\text{A}$ fibers. At high thrombin concentrations these differences between $\gamma\text{A}/\gamma'$ and $\gamma\text{A}/\gamma\text{A}$ fibers largely disappeared.

Using high magnification scanning electron microscopy, we observed a clear difference between $\gamma\text{A}/\gamma'$ and $\gamma\text{A}/\gamma\text{A}$ fibers. Fibers formed with $\gamma\text{A}/\gamma\text{A}$ fibrinogen (Figure 5E, S3) show a more rounded, compacted and robust structure compared with $\gamma\text{A}/\gamma'$ (Figure 5F, Figure S3), at 0.1 U.mL^{-1} thrombin. Furthermore, $\gamma\text{A}/\gamma'$ fibers unravelled into loose structures (Figure 5F, Figure S3). The thin fibrillar structures that are observed in the $\gamma\text{A}/\gamma'$ fibers demonstrate a diameter of $<10 \text{ nm}$, which is consistent with the diameter of individual protofibrils. These data confirm the data obtained by turbidimetric analysis and show that $\gamma\text{A}/\gamma'$ fibers are composed of loosely packed protofibrils that unravel into separate protofibrils in the network at low thrombin concentrations.

$\gamma\text{A}/\gamma'$ fibrin decreases protofibril packing in plasma

To test the effect of $\gamma\text{A}/\gamma'$ on protofibril packing also in plasma we used fibrinogen deficient plasma and supplemented this with purified $\gamma\text{A}/\gamma\text{A}$ fibrinogen, $\gamma\text{A}/\gamma'$ fibrinogen and different ratios of $\gamma\text{A}/\gamma\text{A}:\gamma\text{A}/\gamma'$ fibrinogen; 60%:40% (these relatively high ratios of $\gamma\text{A}/\gamma'$ have previously been observed in healthy subjects³⁸) and 91%:9% (normal ratio and that observed in human plasminogen-depleted IF-1 purified fibrinogen, see Supplement). When adding these fibrinogen mixtures to fibrinogen deficient plasma, we found that for systems supplemented with different

ratios of $\gamma A/\gamma A$ and $\gamma A/\gamma'$ fibrinogen, the radius remained largely similar at each of the thrombin concentrations tested (83.6 ± 2.9 nm for $\gamma A/\gamma A$ and 80.8 ± 0.5 nm for $\gamma A/\gamma'$ at 0.1 U.mL^{-1} ; Figure 6A), in agreement with the data in purified systems (Figure 5A). However, **protofibril numbers** in $\gamma A/\gamma'$ fibrin produced in the plasma milieu were decreased to a similar degree (from 256.5 ± 21.6 to 196.7 ± 3.5 ; $p < 0.05$; Figure 6B), as those of $\gamma A/\gamma'$ fibrin in a purified system at the same thrombin concentration (Figure 5B). Moreover, when we studied fibrinogen mixtures of different $\gamma A/\gamma A:\gamma A/\gamma'$ ratios, significantly decreased **protofibril numbers were** also observed at lower physiological ratios of 40% and 9% $\gamma A/\gamma'$ (Figure 6B). As expected, these changes were associated with **lower protein** density in $\gamma A/\gamma'$ fibers (Figure 6C) and increased space between protofibrils (Figure 6D). At higher thrombin, like in the purified system, protofibril composition was similar between $\gamma A/\gamma A$ and $\gamma A/\gamma'$ (Table S2 and Figure S4).

$\gamma A/\gamma'$ fibrin and clot stiffness

Finally, we studied the effects of $\gamma A/\gamma'$ fibrinogen on plasma clot stiffness using thromboelastometry. Clots produced with fibrinogen deficient plasma supplemented with $\gamma A/\gamma'$ fibrinogen showed reduced maximum clot firmness and storage modulus, while clotting times were increased, compared with $\gamma A/\gamma A$ at low thrombin concentration (Table 2, Figure S5). Interestingly, whereas for $\gamma A/\gamma A$ fibrinogen we found similar effects of increasing thrombin on reducing clot stiffness as in whole blood and normal plasma, increasing thrombin concentrations did not significantly further reduce clot stiffness in clots produced with $\gamma A/\gamma'$ fibrinogen. This is in agreement with a major effect of increasing thrombin on reducing protofibril packing

in clots produced with $\gamma A/\gamma A$ fibrinogen, while the number of protofibrils packed per fibrin fiber is lower, and generally remains low with increasing thrombin, in clots produced with $\gamma A/\gamma'$ fibrinogen (Figure 5).

Discussion

The intrafibrillar structure of fibrin was hitherto poorly understood. Our study shows that high thrombin concentrations lead to reduced protofibril packing in plasma and purified systems. We show that reduced protofibril packing contributes to a reduction in fiber radius after dehydration. Despite the well-characterised inhibitory effect of fibrinogen $\gamma A/\gamma'$ on thrombin and thrombin generation,^{10,39,40} we find that $\gamma A/\gamma'$ also reduces protofibril packing. Finally, we find that reduced protofibril packing is associated with clots that are less stiff. These data indicate that protofibril arrangements represent a major mechanism by which both thrombin and fibrinogen $\gamma A/\gamma'$ regulate clot structure and function (Figure 7).

Electron microscopy has been widely used for measuring fiber diameter due to its high resolution compared with light microscopy.^{11,41-44} However, sample preparation for electron microscopy incurs potential structural modifications. Samples for transmission electron microscopy undergo drying or embedding in epoxy resins, which have a high viscosity and hygroscopicity, followed by preparation of a thin sample using e.g. a microtome, and staining. It has been reported that fibrin fibers are composed of approximately 20% protein and 80% water.⁴⁵ Therefore, the dehydration procedure could lead to contraction of the protofibrils, reducing fiber diameter. Samples for scanning electron microscopy are fixed and subjected to critical point drying to minimise artefacts, however, effects of dehydration on the sample cannot be excluded.

Optical turbidimetry currently represents the best method to analyse fibrin fiber diameter in physiological conditions⁴⁶ and this method was recently optimised by

Yeromonahos and colleagues.⁴⁷ While the method was previously corroborated with X-ray scattering,⁴⁷ it had not yet been validated by microscopy. We used turbidity alongside transmission electron, scanning electron and atomic force microscopy to analyse fiber diameters, and find that size measurements by turbidimetry are on average two times larger than diameters observed with electron microscopy. Low thrombin concentrations result in higher protein density, decreased distance between protofibrils, and less solvent content. Therefore, smaller contraction occurs during the dehydration procedure for electron microscopy, leading to the apparent formation of thicker fibers. As per corollary, high thrombin leads to more aqueous fibers and higher contraction during sample preparation, forming thinner fibers. We also performed atomic force microscopy under fully hydrated conditions, which confirmed the diameter measurements by turbidimetry. However, atomic force microscopy has its own limitations: clots are formed in a thin layer on the mica surface, and hence potentially different from clots used in other measurements. Another limitation is that the atomic force microscope tip may move the fibers during measurements. However, major movements are visible as shifts/line-breaks in the images and these moving fibers were excluded from the analysis. Notwithstanding these limitations, the similarities between fiber measurements obtained by atomic force microscopy and turbidimetry strongly support the aqueous nature of fibrin fibers.

High thrombin concentrations have previously been associated with highly branched fibrin network structures with small pores.^{2,26,27} The effects of thrombin concentration on protofibril packing may contribute to changes in fibrin network structure. A decrease in protofibril packing per fiber will lead to availability of “unused” protofibrils for the generation of additional fibers that branch and interweave to form the

network. Therefore, reduced protofibril packing at high thrombin contributes to increased network complexity and reduced average pore-size. Complex fibrin network structures as those produced with elevated thrombin have been shown to be more resistant to fibrinolysis and thereby increase the risk for thrombosis.^{2,28,29}

When coagulation is triggered with tissue factor, thrombin formation follows after a brief lagphase, exponentially increasing until it reaches a peak, and then slowly decaying as thrombin is inhibited by its natural inhibitors in plasma.⁴⁸ At its peak, thrombin reaches several hundred nM (tens U/ml).⁴⁹ However, clot formation already occurs at <0.2 U/ml thrombin, and the vast majority of thrombin is produced after clotting takes place.³³ Only 0.088 U/ml (0.84 nM) thrombin is required for factor XIII activation, 0.135 U/ml for fibrinopeptide A and 0.177 U/ml for fibrinopeptide B release, 2-3 minutes after initiation of clotting in whole blood.³³ We have analysed thrombin at 0.005–10 U/ml (0.048-96 nM), in close agreement with the range of thrombin concentrations responsible for the conversion of key substrates in tissue factor triggered blood coagulation.³³ However, while in blood clotting thrombin concentrations start around 0.001 U/ml and increase over time, we added fixed thrombin concentrations at the start of each experiment, and incubated for 24 hours to allow for clot formation. This is a potential limitation of our method, but represents the closest resemblance to the physiological situation achievable with our set-up.

A major feature of fibrin fibers is strain-hardening upon extension, thought to be important in resisting blood shear forces.^{50,51} The elastic behaviour of fibrin has been attributed to conversion of the **coiled coil α -helices** to β -strands and partial unfolding of the **γ -chain** C-terminal domain^{45,52,53} However, the physical properties that form

the basis of fibrin mechanics remain largely unknown. Piechocka *et al.*⁵⁴ reported that the bundle-like structure of fibrin fibers is responsible for strain hardening properties of clots. Ryan *et al.* proposed that the balance between fiber size and clot branching determines clot stiffness.⁴³ We find that in addition to these mechanisms, the protofibril content within fibrin fibers are a **possible** major novel mechanism that regulates clot viscoelastic properties. Our data on the effect of thrombin on fibrin clot stiffness are in agreement with those reported by Ryan *et al.*, who also found that increasing thrombin leads to decreased clot stiffness (G').⁴³ **We now find similar effects of high thrombin on clot stiffness in purified systems as well as in plasma and whole blood by thromboelastometry.**

The loss modulus G'' in our **magnetic tweezers** experiments remained similar with increasing thrombin which resulted in an increase of loss tangent (G''/G'). This shows that the balance between viscous and elastic nature shifts towards viscous behaviour with increasing thrombin, whilst overall behaviour remains elastic. Ryan *et al.* previously reported that increased thrombin concentration decreased the loss tangent.⁴³ However, these studies were performed in the absence of calcium. When we repeat experiments in the absence of calcium, we observe a minor, but not significant, decrease in loss tangent with increasing thrombin concentrations (Table S1). It is presently unclear how calcium influences the loss tangent, but our main findings reported here are based on clotting under conditions of physiological calcium concentration. Individual fibrin fibers extend to 300%,⁵⁰ and a similar extension is also possible in whole clots.⁵³ It has been suggested that fibrin extensibility is caused by protofibrils sliding relative to each other.^{54,55} Our data **indicate** that **increased** protofibril packing at low thrombin concentrations increases

resistance to protofibril sliding and hence clot rigidity. A recent report showed that individual fibrin fibers produced with low thrombin were less likely to break when lysed with plasmin compared with fibers produced with high thrombin concentrations.⁵⁶ Our findings of increased protofibril packing at low thrombin also provide a possible explanation for the fact that those fibers are less likely to lyse to breakage point.

Physiological γ -chain splice variation is a major source for fibrinogen heterogeneity.⁸ We find that $\gamma A/\gamma'$ shows lower protofibril packing than $\gamma A/\gamma A$ fibrin at thrombin concentrations $\leq 0.1 \text{ U.mL}^{-1}$ in both purified and plasma solutions. Previous studies reported effects of $\gamma A/\gamma'$ fibrinogen on overall clot structure also at higher thrombin concentrations.^{11,31,32,34} These studies focussed on the early stages of fibrin formation and higher thrombin concentrations were required to allow for timely fibrin formation. In contrast, the effects of $\gamma A/\gamma'$ on protofibril packing were demonstrated after 24 hours, therefore requiring lower thrombin concentrations. Interestingly, while $\gamma A/\gamma'$ has been reported to inhibit thrombin and reduce thrombin generation,^{10,39,40} the effect of $\gamma A/\gamma'$ on protofibril packing is similar to that of *increasing* thrombin concentration, *i.e.* a lowering of the number of protofibrils packed per fiber. This indicates that the effects of $\gamma A/\gamma'$ on fiber structure are not caused by thrombin inhibition, but due to other mechanisms. It has previously been reported that the γ' -chain disrupts polymerization due to electrostatic or steric interference.^{31,34} Repulsive forces disrupting polymerization may reduce protofibril packing and increase intra-*protofibrillar* space. The average $\gamma A/\gamma'$ concentration is about 8-15% of total fibrinogen in normal plasma, and this may reach 40%.^{6,8,38} If we reconstitute fibrinogen deficient plasma with fibrinogen mixtures, also a *physiological* range of

$\gamma A/\gamma A:\gamma A/\gamma'$ ratios (from normal to top end) decrease protofibril packing. Therefore, intrafibrillar protofibril arrangements likely play a major role in the patho-physiological effects of fibrinogen $\gamma A/\gamma'$. Furthermore, we show that the intrafibrillar arrangements in $\gamma A/\gamma'$ reconstituted plasma also leads to less stiff clots compared to the $\gamma A/\gamma A$ reconstituted plasma. This occurs only at thrombin concentrations where significant differences in protofibril number between the two systems exist.

In conclusion, we demonstrate that protofibril content of fibrin fibers is determined by thrombin concentration and fibrinogen γ' . Protofibril packing is closely associated with clot mechanical properties, whereby fibrin rigidity is increased with higher protofibril content, leading to enhanced fiber compactness. These findings show a major role for protofibril packing in the regulation of clot structure and fibrin elastic properties, thereby influencing clot strength and potentially the risk for thrombosis or thrombus embolisation.

Acknowledgements

This study was supported by the British Heart Foundation (RG/13/3/30104).

Authorship: MMD, CD and FLM performed experiments; MMD, CD, FLM, SDC and RASA analysed the results and made the figures; HRM, KIB, RAA, VCR and HP contributed to discussion and interpretation of the data; All authors read and approved the final manuscript; MMD, SDC and RASA designed the research and wrote the paper.

Conflict-of-interest disclosure: The authors declare no competing financial interests.

References

1. Lord ST. Molecular mechanisms affecting fibrin structure and stability. *Arterioscler Thromb Vasc Biol.* 2011;31(3):494-499.
2. Wolberg AS. Thrombin generation and fibrin clot structure. *Blood Rev.* 2007;21(3):131-142.
3. Brown JH, Volkmann N, Jun G, Henschen-Edman AH, Cohen C. The crystal structure of modified bovine fibrinogen. *Proc Natl Acad Sci U S A.* 2000;97(1):85-90.
4. Doolittle RF, Yang Z, Mochalkin I. Crystal structure studies on fibrinogen and fibrin. *Ann N Y Acad Sci.* 2001;936:31-43.
5. Yang Z, Kollman JM, Pandi L, Doolittle RF. Crystal structure of native chicken fibrinogen at 2.7 Å resolution. *Biochemistry.* 2001;40(42):12515-12523.
6. Chung DW, Davie EW. gamma and gamma' chains of human fibrinogen are produced by alternative mRNA processing. *Biochemistry.* 1984;23(18):4232-4236.
7. Francis CW, Marder VJ. Heterogeneity of normal human fibrinogen due to two high molecular weight variant gamma chains. *Ann N Y Acad Sci.* 1983;408:118-120.
8. Wolfenstein-Todel C, Mosesson MW. Carboxy-terminal amino acid sequence of a human fibrinogen gamma-chain variant (gamma'). *Biochemistry.* 1981;20(21):6146-6149.
9. Chan HH, Leslie BA, Stafford AR, et al. By increasing the affinity of heparin for fibrin, Zn(2+) promotes the formation of a ternary heparin-thrombin-fibrin complex that protects thrombin from inhibition by antithrombin. *Biochemistry.* 2012;51(40):7964-7973.
10. de Bosch NB, Mosesson MW, Ruiz-Saez A, Echenagucia M, Rodriguez-Lemoin A. Inhibition of thrombin generation in plasma by fibrin formation (Antithrombin I). *Thromb Haemost.* 2002;88(2):253-258.
11. Cooper AV, Standeven KF, Ariens RA. Fibrinogen gamma-chain splice variant gamma' alters fibrin formation and structure. *Blood.* 2003;102(2):535-540.
12. Cheung EY, Uitte de Willige S, Vos HL, et al. Fibrinogen gamma' in ischemic stroke: a case-control study. *Stroke.* 2008;39(3):1033-1035.

13. Lovely RS, Falls LA, Al-Mondhiry HA, et al. Association of gammaA/gamma' fibrinogen levels and coronary artery disease. *Thromb Haemost.* 2002;88(1):26-31.
14. Mannila MN, Lovely RS, Kazmierczak SC, et al. Elevated plasma fibrinogen gamma' concentration is associated with myocardial infarction: effects of variation in fibrinogen genes and environmental factors. *J Thromb Haemost.* 2007;5(4):766-773.
15. Mosesson MW, Hernandez I, Raife TJ, et al. Plasma fibrinogen gamma' chain content in the thrombotic microangiopathy syndrome. *J Thromb Haemost.* 2007;5(1):62-69.
16. Uitte de Willige S, de Visser MC, Houwing-Duistermaat JJ, Rosendaal FR, Vos HL, Bertina RM. Genetic variation in the fibrinogen gamma gene increases the risk for deep venous thrombosis by reducing plasma fibrinogen gamma' levels. *Blood.* 2005;106(13):4176-4183.
17. Veklich YI, Gorkun OV, Medved LV, Nieuwenhuizen W, Weisel JW. Carboxyl-terminal portions of the alpha chains of fibrinogen and fibrin. Localization by electron microscopy and the effects of isolated alpha C fragments on polymerization. *J Biol Chem.* 1993;268(18):13577-13585.
18. Litvinov RI, Yakovlev S, Tsurupa G, Gorkun OV, Medved L, Weisel JW. Direct evidence for specific interactions of the fibrinogen alphaC-domains with the central E region and with each other. *Biochemistry.* 2007;46(31):9133-9142.
19. Medved L, Weisel JW, and on behalf of fibrinogen and factor XIII subcommittee of the scientific standardization committee of the international society on thrombosis and haemostasis. Recommendations for nomenclature on fibrinogen and fibrin. *J Thromb Haemost.* 2009;7(2):355-359.
20. Nair CH, Shah GA, Dhall DP. Effect of temperature, pH and ionic strength and composition on fibrin network structure and its development. *Thromb Res.* 1986;42(6):809-816.
21. Glover CJ, McIntire LV, Brown CH, 3rd, Natelson EA. Rheological properties of fibrin clots. Effects of fibrinogen concentration, Factor XIII deficiency, and Factor XIII inhibition. *J Lab Clin Med.* 1975;86(4):644-656.

22. Duval C, Allan P, Connell SD, Ridger VC, Philippou H, Ariens RA. Roles of fibrin alpha- and gamma-chain specific cross-linking by FXIIIa in fibrin structure and function. *Thromb Haemost.* 2014;111(5):842-850.
23. Hethershaw EL, Cilia La Corte AL, Duval C, et al. The effect of blood coagulation factor XIII on fibrin clot structure and fibrinolysis. *J Thromb Haemost.* 2014;12(2):197-205.
24. Kurniawan NA, Grimbergen J, Koopman J, Koenderink GH. Factor XIII stiffens fibrin clots by causing fiber compaction. *J Thromb Haemost.* 2014;12(10):1687-1696.
25. Carr ME, Jr., Gabriel DA, McDonagh J. Influence of Ca²⁺ on the structure of reptilase-derived and thrombin-derived fibrin gels. *Biochem J.* 1986;239(3):513-516.
26. Blomback B, Carlsson K, Fatah K, Hessel B, Procyk R. Fibrin in human plasma: gel architectures governed by rate and nature of fibrinogen activation. *Thromb Res.* 1994;75(5):521-538.
27. Blomback B, Carlsson K, Hessel B, Liljeborg A, Procyk R, Aslund N. Native fibrin gel networks observed by 3D microscopy, permeation and turbidity. *Biochim Biophys Acta.* 1989;997(1-2):96-110.
28. Wolberg AS, Monroe DM, Roberts HR, Hoffman M. Elevated prothrombin results in clots with an altered fiber structure: a possible mechanism of the increased thrombotic risk. *Blood.* 2003;101(8):3008-3013.
29. Undas A, Ariens RA. Fibrin clot structure and function: a role in the pathophysiology of arterial and venous thromboembolic diseases. *Arterioscler Thromb Vasc Biol.* 2011;31(12):e88-99.
30. Wolberg AS. Determinants of fibrin formation, structure, and function. *Curr Opin Hematol.* 2012;19(5):349-356.
31. Gersh KC, Nagaswami C, Weisel JW, Lord ST. The presence of gamma' chain impairs fibrin polymerization. *Thromb Res.* 2009;124(3):356-363.
32. Siebenlist KR, Mosesson MW, Hernandez I, et al. Studies on the basis for the properties of fibrin produced from fibrinogen-containing gamma' chains. *Blood.* 2005;106(8):2730-2736.

33. Brummel KE, Paradis SG, Butenas S, Mann KG. Thrombin functions during tissue factor-induced blood coagulation. *Blood*. 2002;100(1):148-152.
34. Allan P, Uitte de Willige S, Abou-Saleh RH, Connell SD, Ariens RA. Evidence that fibrinogen gamma' directly interferes with protofibril growth: implications for fibrin structure and clot stiffness. *J Thromb Haemost*. 2012;10(6):1072-1080.
35. Abou-Saleh RH, Connell SD, Harrand R, et al. Nanoscale probing reveals that reduced stiffness of clots from fibrinogen lacking 42 N-terminal Bbeta-chain residues is due to the formation of abnormal oligomers. *Biophys J*. 2009;96(6):2415-2427.
36. Evans RM, Tassieri M, Auhl D, Waigh TA. Direct conversion of rheological compliance measurements into storage and loss moduli. *Phys Rev E Stat Nonlin Soft Matter Phys*. 2009;80(1 Pt 1):012501.
37. Blinc A, Magdic J, Fric J, Musevic I. Atomic force microscopy of fibrin networks and plasma clots during fibrinolysis. *Fibrinolysis & Proteolysis*. 2000;14(5):288-299.
38. Pieters M, Kotze RC, Jerling JC, Kruger A, Ariens RA. Evidence that fibrinogen gamma' regulates plasma clot structure and lysis and relationship to cardiovascular risk factors in black Africans. *Blood*. 2013;121(16):3254-3260.
39. Lovely RS, Boshkov LK, Marzec UM, Hanson SR, Farrell DH. Fibrinogen gamma' chain carboxy terminal peptide selectively inhibits the intrinsic coagulation pathway. *Br J Haematol*. 2007;139(3):494-503.
40. Omarova F, Uitte De Willige S, Ariens RA, Rosing J, Bertina RM, Castoldi E. Inhibition of thrombin-mediated factor V activation contributes to the anticoagulant activity of fibrinogen gamma'. *J Thromb Haemost*. 2013;11(9):1669-1678.
41. Collet JP, Moen JL, Veklich YI, et al. The alphaC domains of fibrinogen affect the structure of the fibrin clot, its physical properties, and its susceptibility to fibrinolysis. *Blood*. 2005;106(12):3824-3830.
42. Gorkun OV, Veklich YI, Weisel JW, Lord ST. The conversion of fibrinogen to fibrin: recombinant fibrinogen typifies plasma fibrinogen. *Blood*. 1997;89(12):4407-4414.
43. Ryan EA, Mockros LF, Weisel JW, Lorand L. Structural origins of fibrin clot rheology. *Biophysical Journal*. 1999;77(5):2813-2826.

44. Veklich Y, Francis CW, White J, Weisel JW. Structural studies of fibrinolysis by electron microscopy. *Blood*. 1998;92(12):4721-4729.
45. Lim BB, Lee EH, Sotomayor M, Schulten K. Molecular basis of fibrin clot elasticity. *Structure*. 2008;16(3):449-459.
46. Carr ME, Jr., Hermans J. Size and density of fibrin fibers from turbidity. *Macromolecules*. 1978;11(1):46-50.
47. Yeromonahos C, Polack B, Caton F. Nanostructure of the fibrin clot. *Biophys J*. 2010;99(7):2018-2027.
48. Hemker HC, Giesen PL, Ramjee M, Wagenvoort R, Beguin S. The thrombogram: monitoring thrombin generation in platelet-rich plasma. *Thromb Haemost*. 2000;83(4):589-591.
49. Mann KG. Thrombin formation. *Chest*. 2003;124(3 Suppl):4S-10S.
50. Liu W, Jawerth LM, Sparks EA, et al. Fibrin fibers have extraordinary extensibility and elasticity. *Science*. 2006;313(5787):634.
51. Shah JV, Janmey PA. Strain hardening of fibrin gels and plasma clots. *Rheologica Acta*. 1997;36(3):262-268.
52. Guthold M, Liu W, Sparks EA, et al. A comparison of the mechanical and structural properties of fibrin fibers with other protein fibers. *Cell Biochem Biophys*. 2007;49(3):165-181.
53. Brown AE, Litvinov RI, Discher DE, Purohit PK, Weisel JW. Multiscale mechanics of fibrin polymer: gel stretching with protein unfolding and loss of water. *Science*. 2009;325(5941):741-744.
54. Piechocka IK, Bacabac RG, Potters M, Mackintosh FC, Koenderink GH. Structural hierarchy governs fibrin gel mechanics. *Biophys J*. 2010;98(10):2281-2289.
55. Houser JR, Hudson NE, Ping L, et al. Evidence that alphaC region is origin of low modulus, high extensibility, and strain stiffening in fibrin fibers. *Biophys J*. 2010;99(9):3038-3047.
56. Bucay I, O'Brien ET, 3rd, Wulfe SD, et al. Physical determinants of fibrinolysis in single fibrin fibers. *PLoS One*. 2015;10(2):e0116350.

Table

Table 1 – Viscoelastic properties of fibrin clots produced with human plasminogen-depleted IF-1 purified fibrinogen.

[Thrombin], U.mL ⁻¹	G' , Pa	G'' , Pa	$\tan \delta$
0.1	0.677±0.046	0.164±0.010	0.242±0.022
1.0	0.360±0.051**	0.255±0.021	0.708±0.116*
5.0	0.259±0.034****	0.126±0.072	0.486±0.285

Data represented as mean ± SD, n=3. Statistical significance is denoted with * p<0.05, ** p<0.01, and **** p<0.001, for comparison between 0.1 U.mL⁻¹ and the remaining thrombin concentrations.

Table 2 – Thromboelastometric properties of fibrin clots produced with whole blood, normal pooled plasma and fibrinogen deficient plasma supplemented with γ A/ γ A and γ A/ γ ' fibrinogen.

	Whole Blood		Normal Pooled Plasma		Fibrinogen Deficient Plasma			
					γ A/ γ A		γ A/ γ '	
[Thrombin] (U.mL ⁻¹)	1.0	10.0	1.0	10.0	1.0	10.0	1.0	10.0
MCF (mm)	60.0±3.6	36.0±11.1*	25.7±3.0	11.2±3.3*	20.5±1.3	13.7±4.2*	12.7±0.6 [#]	11.3±2.1
G (×10 ³ , dyne.cm ⁻²)	7.7±1.1	3.0±1.3*	1.7±0.3	0.6±0.2*	1.3±0.1	0.8±0.3*	0.7±0.0 [#]	0.6±0.1
CT (s)	81.5±27.6	46.0±27.7	76.7±23.9	19.8±10.5*	131.3±29.3	11.7±5.9*	204.3±8.7 [#]	13.7±5.5*
CFR (°)	65.0±5.6	59.7±6.4	53.3±8.0	58.3±4.1	58.5±1.7	71.0±10.4	44.0±5.3	59.3±6.5

Data represented as mean ± SD, n=3. Statistical significance is denoted with * p<0.05, for differences between 1.0 and 10.0 U.mL⁻¹ thrombin; and [#] p<0.05, for comparison between γ A/ γ A and γ A/ γ ' supplemented fibrinogen deficient plasmas with the same thrombin concentration. MCF: Maximum Clot Firmness; G: Storage Modulus; CT: Clot formation time; CFR: Clot formation rate

Figure Legends

Figure 1 – Thrombin effects on fibrin clot network and fibrin fiber size.

Transmission electron microscopy pictures under dried conditions of fibrin clots made with human plasminogen-depleted IF-1 purified fibrinogen (1 mg.mL⁻¹), CaCl₂ (2.5 mM) and thrombin at concentrations of A) 0.1 U.mL⁻¹; B) 1.0 U.mL⁻¹; and C) 10 U.mL⁻¹. The scale-bar in each picture corresponds to 500 nm. D) Fibrin fiber radius obtained by measurement of **n=50** fibrin fibers at 0.1 U.mL⁻¹, 1.0 U.mL⁻¹ and 10 U.mL⁻¹ thrombin. The individually plotted data represent the dispersion of the fiber size within the clot and the bar represents the mean value. Statistical significance, using a one-way ANOVA, are denoted with **** p<0.001 for comparison between 0.1 U.mL⁻¹ and the remaining thrombin concentrations.

Figure 2 – Thrombin effects on molecular structure of fibrin fibers in purified systems.

Clots were made with human plasminogen-depleted IF-1 purified fibrinogen (1 mg.mL⁻¹), thrombin (0.005-10 U.mL⁻¹) and CaCl₂ (2.5 mM) and analysed by turbidimetry. A) Fibrin fiber radius; B) Number of protofibrils within fibrin fiber; C) Protein density of fibrin fibers; D) Distance between protofibrils inside of fibrin fibers. The results represent the mean values ± **SD, n=3**. Statistical significance, using a one-way ANOVA, are denoted with ** p<0.01, *** p<0.005 and **** p<0.001 for comparison between 0.005 U.mL⁻¹ and the remaining thrombin concentrations.

Figure 3 – Thrombin effects on molecular structure of fibrin fibers in plasma.

Clots were made with normal pooled human plasma (0.3 mg.mL⁻¹), thrombin (0.1 and 1.0 U.mL⁻¹) and CaCl₂ (10 mM) and analysed by turbidimetry. A) Fibrin fiber

radius; B) Number of protofibrils within **the** fibrin fiber; C) Protein density of fibrin fibers; D) Distance between protofibrils inside **the** fibrin fibers. The results represent the mean values \pm **SD, n=3**. Statistical significance, using an unpaired t-test, are denoted with *** $p < 0.005$ and **** $p < 0.001$ for comparison.

Figure 4 – Thrombin effects on fibrin fiber size by atomic force microscopy. A) 3 representative atomic force microscopy images of fibrin fibers formed with human plasminogen-depleted IF-1 purified fibrinogen (1 mg.mL^{-1}), 2.5 mM CaCl_2 and 0.1 , 1.0 and 10 U.mL^{-1} thrombin; B) Fibrin fiber radius obtained by atomic force microscopy in liquid at 0.1 , 1.0 and 10 U.mL^{-1} thrombin. Each image is $4 \times 4 \text{ }\mu\text{m}$, the scale bar indicates 500 nm , and five cross sections along the fibrin fiber are shown that were used in fiber diameter calculations. The results represent the mean values \pm **SD, n=25 fibers**. Statistical significance, using a one-way ANOVA, are denoted with *** $p < 0.005$ and **** $p < 0.001$ for comparison between 0.1 U.mL^{-1} and the remaining thrombin concentrations.

Figure 5 – Effect of γ' on the molecular structure of fibrin fibers over a range of thrombin concentrations. Fibrin was made with 1 mg.mL^{-1} purified $\gamma\text{A}/\gamma\text{A}$ (white bars) or $\gamma\text{A}/\gamma'$ (black bars) fibrinogen, 2.5 mM CaCl_2 and a range of thrombin concentrations. A) Fibrin fiber radius; B) Number of protofibrils within fibrin fibers; C) Protein density of fibrin fibers; D) Distance between protofibrils inside the fibrin fibers. E) **Scanning electron image of $\gamma\text{A}/\gamma\text{A}$ fibrin fibers at thrombin 0.1 U.mL^{-1}** ; F) **Scanning electron image of $\gamma\text{A}/\gamma'$ fibrin fibers at thrombin 0.1 U.mL^{-1}** (scale bars indicate 200 nm); I) Polyacrylamide gel electrophoresis of fibrinogen. Lane 1: molecular marker (kDa); Lane 2: $\gamma\text{A}/\gamma\text{A}$ fibrinogen; Lane 3: $\gamma\text{A}/\gamma'$ fibrinogen; Lane 4:

human plasminogen-depleted IF-1 purified fibrinogen. The results represent the mean values \pm SD, n=3. Statistical significance, using a two-way ANOVA, are denoted with, *** $p < 0.005$ and **** $p < 0.001$ for comparison between $\gamma A/\gamma A$ and $\gamma A/\gamma'$ at each thrombin concentrations.

Figure 6 – Effect of γ' on the molecular structure of fibrin fibers in plasma.

Fibrinogen deficient plasma was diluted 1/10 and supplemented with 0.3 mg.mL^{-1} of purified $\gamma A/\gamma A$ (white bars), $\gamma A/\gamma'$ (black bars), $\gamma A/\gamma A:\gamma A/\gamma'$ 60%:40% (grey bars) and $\gamma A/\gamma A:\gamma A/\gamma'$ 91%:9% (square patterned bars) fibrinogen, 10 mM CaCl_2 and thrombin concentration of 0.1 U.mL^{-1} . A) Fibrin fiber radius; B) Number of protofibrils within fibrin fibers; C) Protein density of fibrin fibers; D) Distance between protofibrils inside the fibrin fibers. The results represent the mean values \pm SD, n=3. Statistical significance, using a one-way ANOVA, are denoted with, * $p < 0.05$, ** $p < 0.01$, *** $p < 0.005$ and **** $p < 0.001$ for comparison between $\gamma A/\gamma A$ and the other fibrinogen systems. The quantitative data is presented in Table S2.

Figure 7 – Schematic representation of the effects of thrombin and γ' on hydrated fibrin fibers. Increased thrombin concentration, as well as replacement of $\gamma A/\gamma A$ by $\gamma A/\gamma'$, leads to formation of less compact fibrin fibers with lower protein density. This is associated with mechanical weakness of fibrin fibers under bloodstream shear.

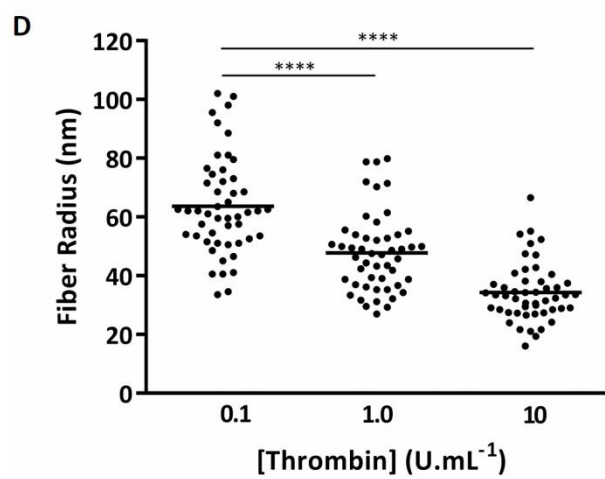
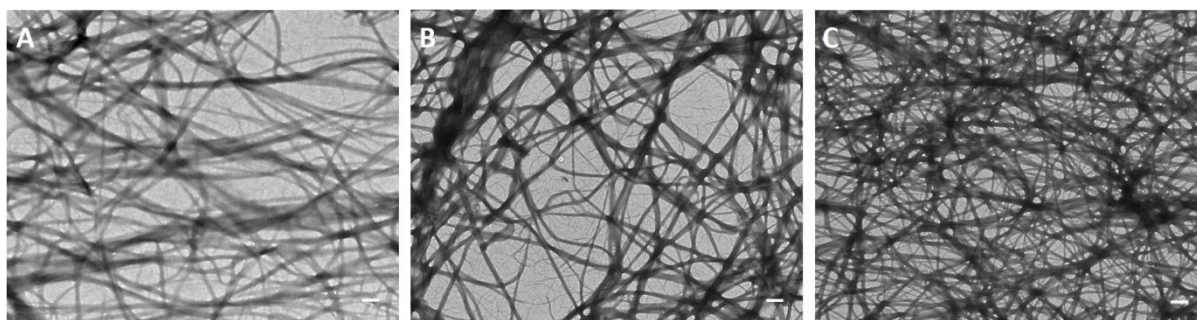
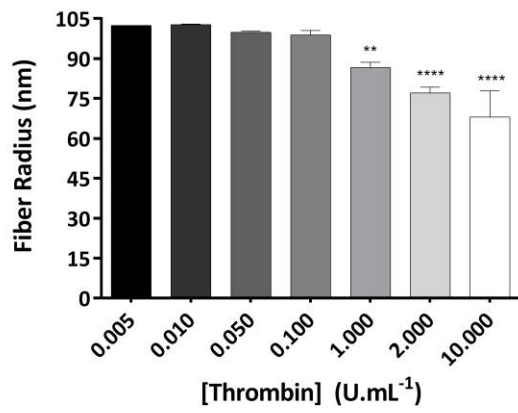
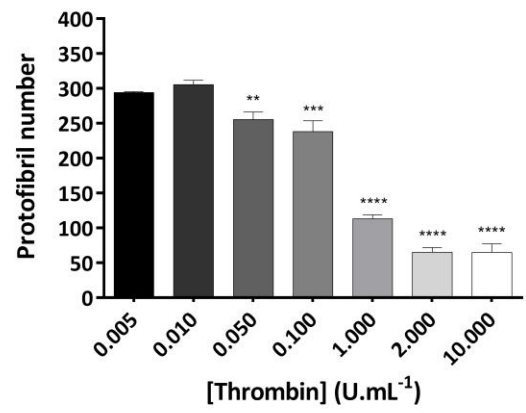
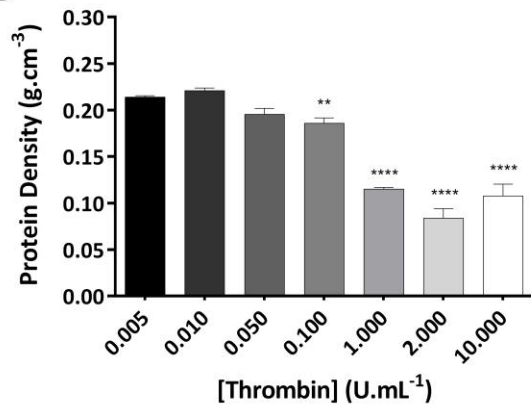
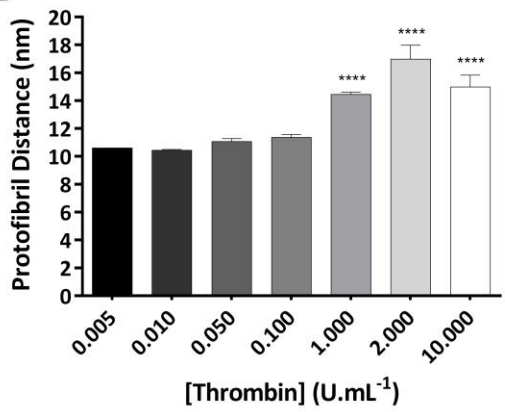


Figure 1

A**B****C****D****Figure 2**

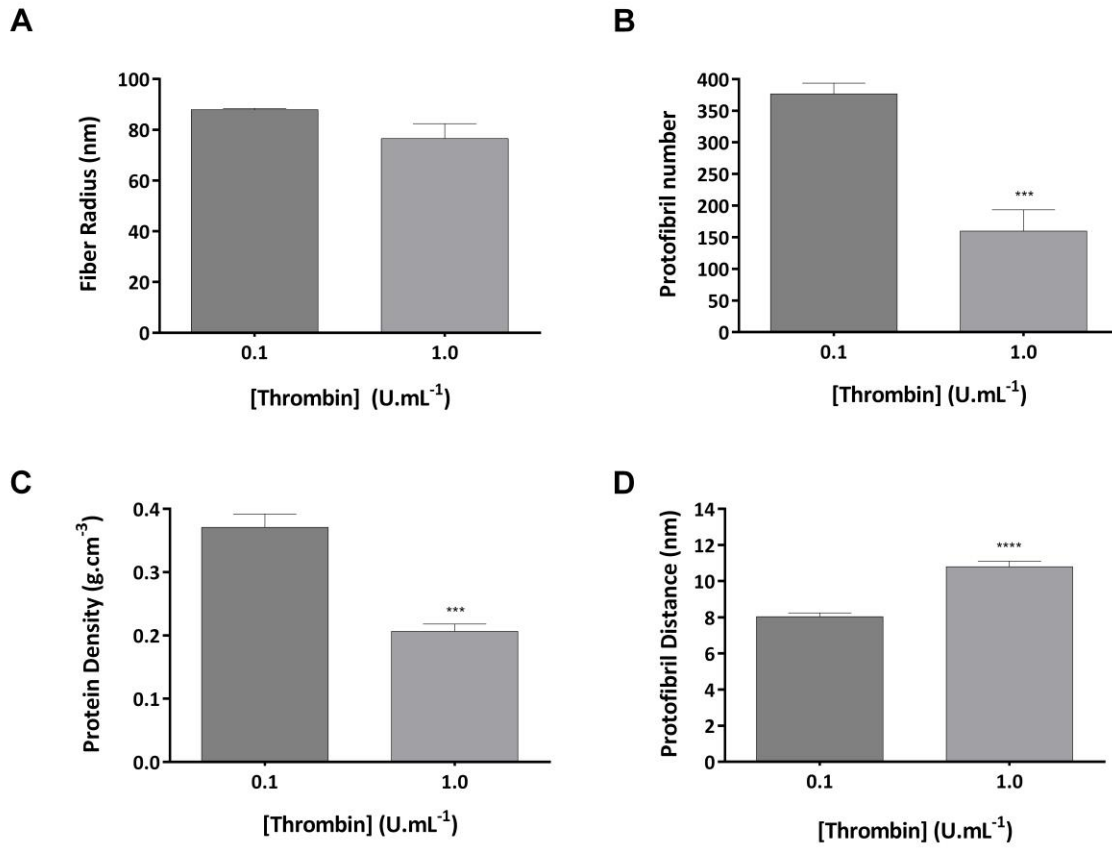


Figure 3

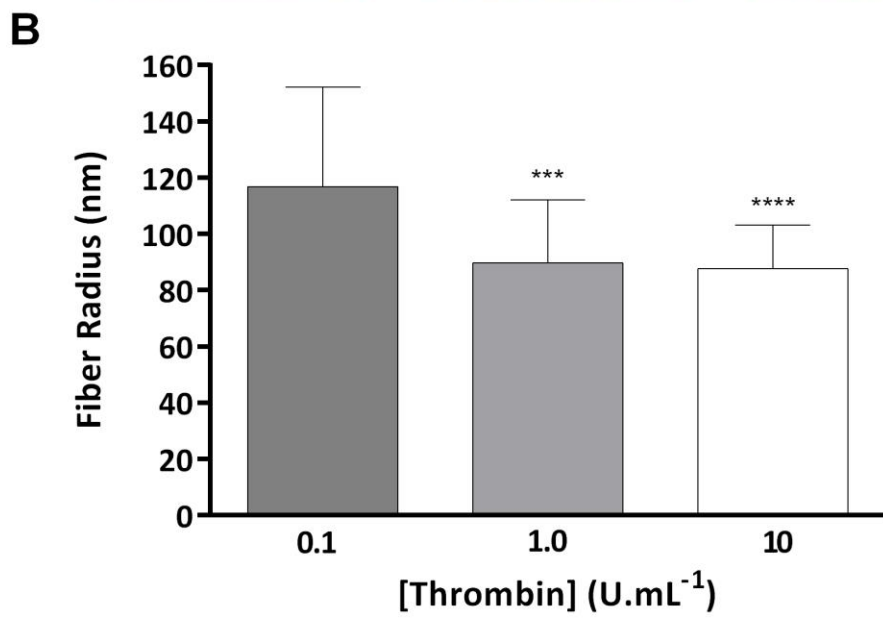
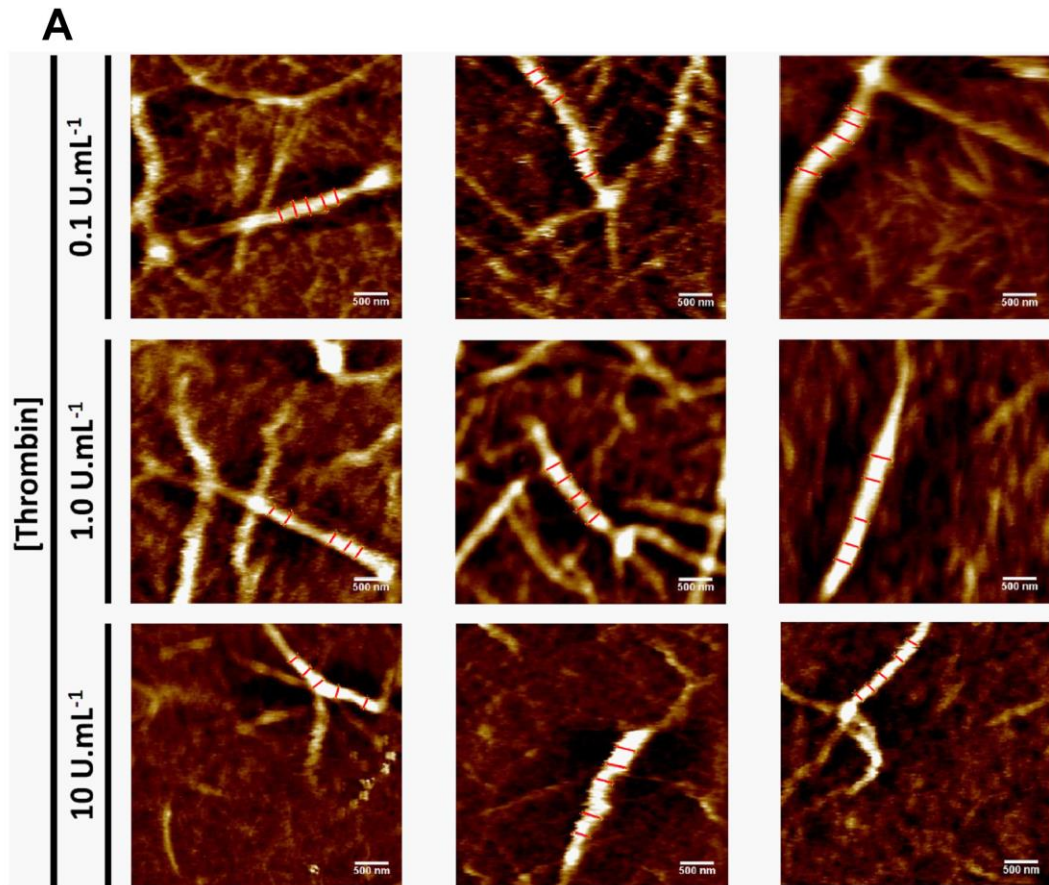


Figure 4

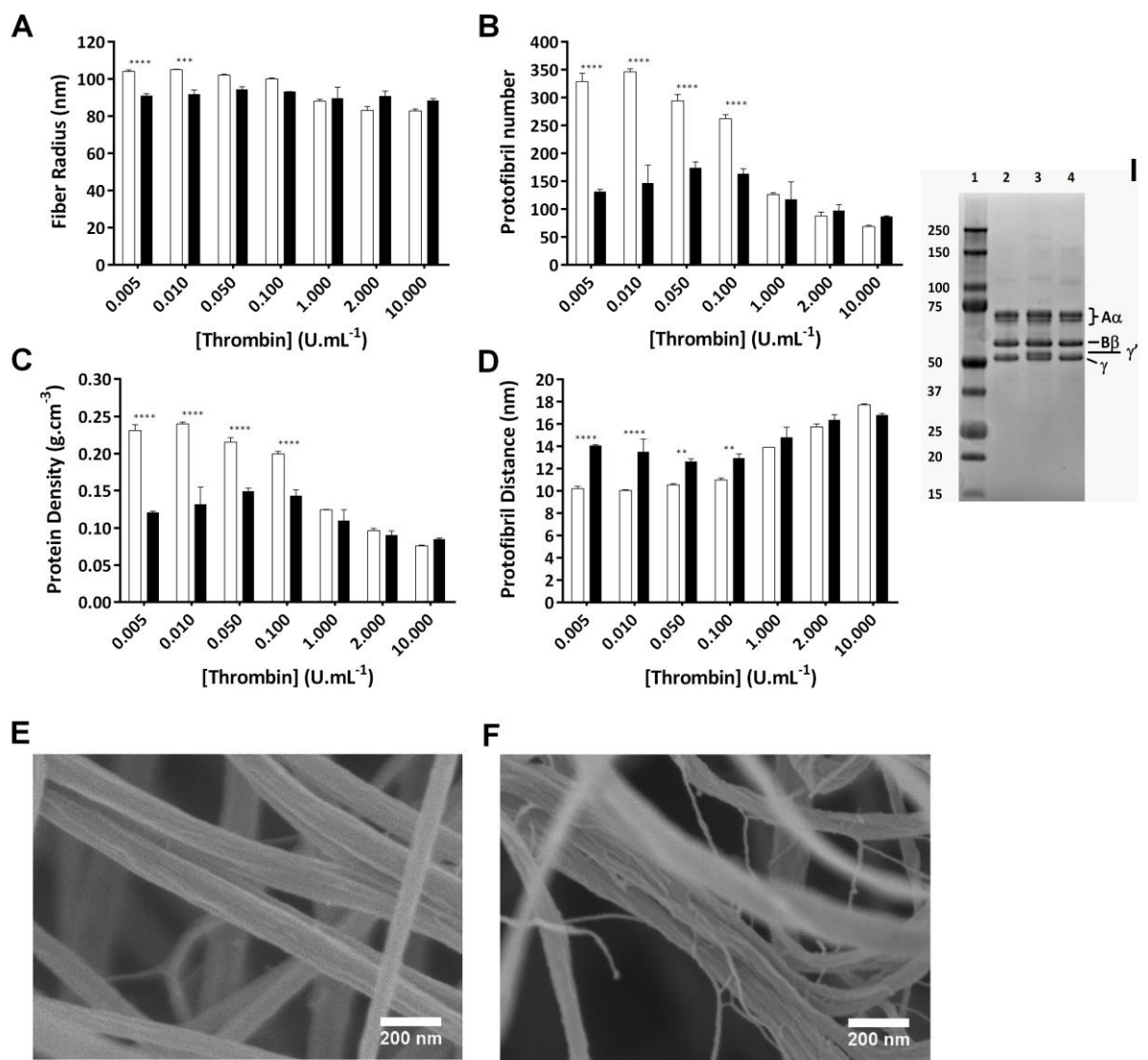


Figure 5

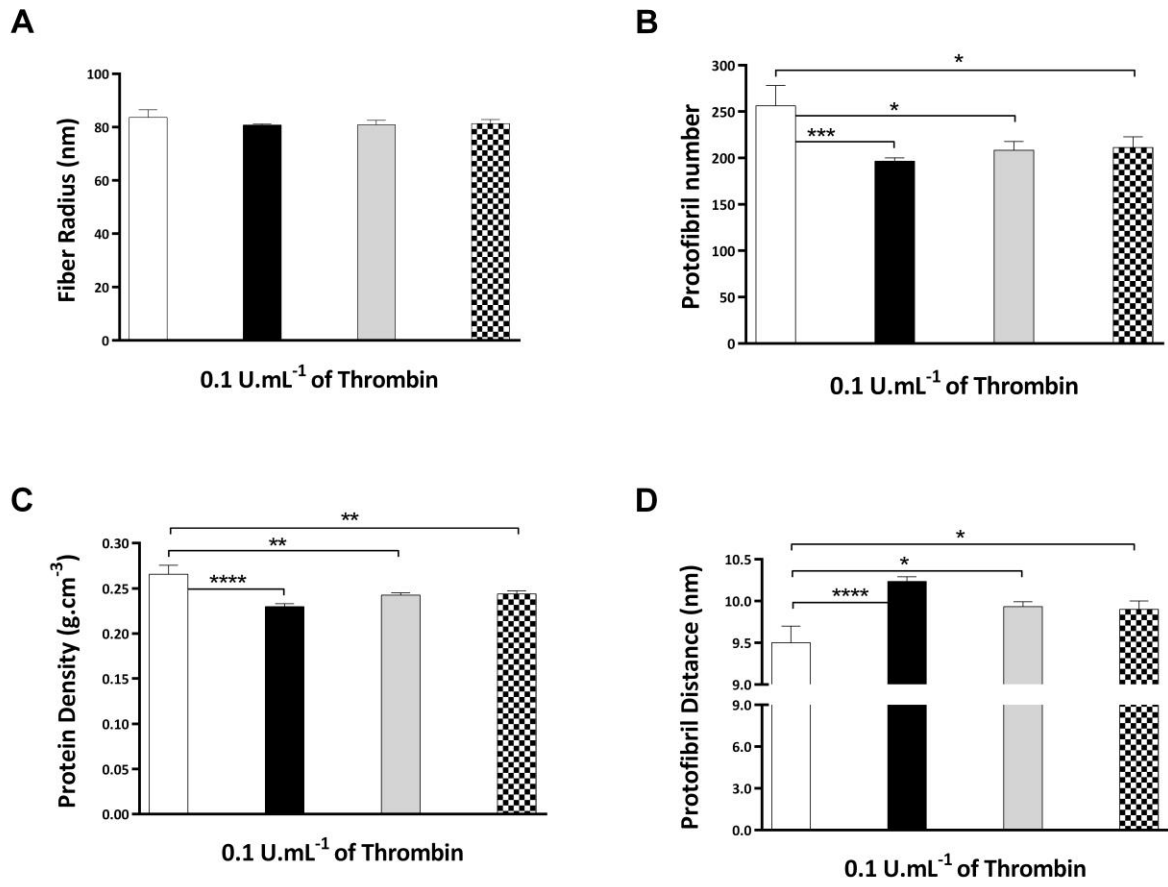
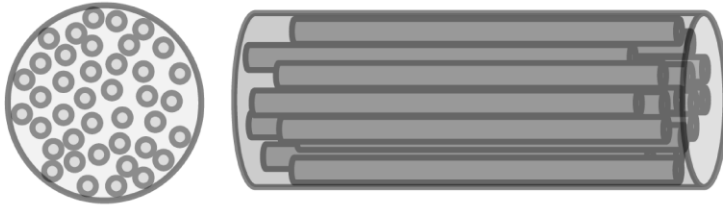


Figure 6

Low thrombin or $\gamma A/\gamma'$



- Increased protofibril packing
- Stiff fibrin fiber



High thrombin or $\gamma A/\gamma'$



- Decreased protofibril packing
- Less stiff fibrin fiber

Figure 7